A long DNA segment in a linear nanoscale Paul trap

Sony Joseph[1]**, Weihua Guan**[2]**, Mark A Reed**[2,3]
and Predrag S Krstic[1,4]

[1] Physics Division, Oak Ridge National Laboratory, PO Box 2008, Oak Ridge, TN 37831, USA
[2] Department of Electrical Engineering, Yale University, New Haven, CT 06520, USA
[3] Department of Applied Physics, Yale University, New Haven, CT 06520, USA

E-mail: krsticp@ornl.gov

Abstract

We study the dynamics of a linearly distributed line charge such as single stranded DNA (ssDNA) in a nanoscale, linear 2D Paul trap in vacuum. Using molecular dynamics simulations we show that a line charge can be trapped effectively in the trap for a well defined range of stability parameters. We investigated (i) a flexible bonded string of charged beads and (ii) a ssDNA polymer of variable length, for various trap parameters. A line charge undergoes oscillations or rotations as it moves, depending on its initial angle, the position of the center of mass and the velocity. The stability region for a strongly bonded line of charged beads is similar to that of a single ion with the same charge to mass ratio. Single stranded DNA as long as 40 nm does not fold or curl in the Paul trap, but could undergo rotations about the center of mass. However, we show that a stretching field in the axial direction can effectively prevent the rotations and increase the confinement stability.

(Some figures in this article are in colour only in the electronic version)

1. Introduction

A quadrupole Paul trap is commonly used either for trapping ions or for mass selective spectrometry. The trap appears in both linear (2D) and 3D varieties, and its dynamical confinement functions are in general characterized by a combination of a DC and an AC (rf) electric fields and rf frequency, by the trap dimensions and by mass and charge of the confined ions (Paul 1990). The most known application of the linear Paul trap is for mass analysis of ions being a component of a quadrupole mass spectrometer. An excellent review of the functions and applications of the conventional Paul ion traps is given by Leibfried *et al* (Leibfried *et al* 2003). More recent applications of the Paul traps are for quantum information processing (Vant *et al* 2006, Seidelin *et al* 2006), for coherent quantum-state manipulation of trapped atomic ions (Wineland *et al* 1998), for functional studies with fluorescent proteins (Rothbauer *et al* 2008), for laser sideband cooling of the motion (Abich *et al* 2004), for formation of ordered structures of trapped ions (Schiffer 2003, Shi *et al*

1999, Itano *et al* 1995, Walther 1995, Edwards *et al* 1994), etc.

Currently there is considerable interest in studying properties of macromolecules and biomolecules. The idea of a fast and cheap DNA sequencing by measuring transversal current while the DNA is translocating through a nanogap or a nanopore has directly motivated the present work (Branton *et al* 2008). Approaches to a DNA sequencing using synthetic nanopores have been recently reviewed (Rhee and Burns 2006, 2007, Branton *et al* 2008). Nanopores can be an effective tool for confinement of a DNA (Aksimentiev *et al* 2004a, 2004b, Chen 2005, Fredlake *et al* 2006, Healy 2007, Kricka *et al* 2005, Nakane *et al* 2003, Ryan *et al* 2007, Zhao *et al* 2007, Payne *et al* 2008), while the translocating DNA efficiently mask ionic current through the pore, specific of a nucleotide instantaneously in the pore (Kasianowicz *et al* 1996, Howorka *et al* 2001). Alternatively, a tunneling current measured across the pore transversally to the translocating DNA varies with a base passing the pore (Zwolak and Di Ventra 2005, Zikic *et al* 2006, Zhang *et al* 2006, Lagerqvist *et al* 2006). However, it has been realized that repeatable measurements of the base specific

---

[4] Author to whom any correspondence should be addressed.

signature of each nucleotide depends critically on its difficult to control relative geometry to the pore during the DNA sequencing (Lagerqvist *et al* 2007, Tabard-Cossa *et al* 2007). For example, it is found that the variation in the conductance due to the geometry of the base relative the electrode can easily override the difference between different types of nucleotide (Zhang *et al* 2006, Zikic *et al* 2006). Therefore, a full control of the DNA translocation and localization as it threads the nanopore becomes a primary concern for the DNA sequencing techniques using synthetic nanopores (Trepagnier *et al* 2007, Tsai and Chen 2007, Chen and Peng 2003). The novel idea of confinement of an ion in an aqueous environment within a Paul-type quadrupole trap (Zhao and Krstic 2008) offers increased electrical detection efficiency for heteropolymers confined within a nanopore regardless of detection scheme (Arnott *et al* 1998, Oberacher *et al* 2004). A ssDNA polymer is negatively charged along its phosphorous backbone, with one elementary charge per a monomer. Thus charged DNA can be stabilized by a combined static and rf quadrupole trapping electric fields in a linear Paul trap, which control its translocation through the device. Thus, the poor signal-to-noise ratio in measuring of the transversal tunneling currents which is partially caused by the inadequate stabilization of motion and localization of the DNA in the nanopore, is expected to be significantly improved by combination of a nanopore with Paul nanotrap.

Though Paul trap has been generally used for trapping single ions in vacuum, recent molecular simulations have demonstrated that a nanoscale quadrupole Paul trap is capable of effectively confining ionic particles in both vacuum and in an aqueous environment (Zhao and Krstic 2008). Such environment might be crucial for supporting the trap functions for biomolecular ions like DNA. However, DNA appears more like a filamentous distribution of charge than a particle. The main goal of this work is to demonstrate, using a series of molecular dynamics simulations, confinement and dynamics of a linear bounded system of charges, ssDNA in particular, in a linear Paul nanotrap in vacuum, while aqueous environment is subject of our future work. The specific details of the Paul trap parameters and MD methods are given in sections 2 and 3 respectively. The results of the simulations are presented in section 4, We first study confinement of a line charge, constructed as a chain of charged beads bound by harmonic forces of various strengths, followed by the study of ssDNA of the various nucleotide types. Section 5 contains our conclusions.

2. System setup for 2D trap

In a quadrupole trap, the electric potential has the form (Leibfried *et al* 2003)

$$\Phi(r, z, t) = \frac{\Phi_0}{2r_0^2}(\alpha x^2 + \beta y^2 + \gamma z^2) \qquad (1)$$

with the constraint $\alpha + \beta + \gamma = 0$ to satisfy the Laplace equation $\nabla^2 \Phi = 0$ at all times. The 3D trap itself generally consists of two hyperbolic metal electrodes with their foci facing each other and a hyperbolic ring electrode halfway

between the other two electrodes. The ions are trapped in the space between these three electrodes by a combination of AC and DC electric fields. A linear (2D) Paul trap is composed of four cylindrically shaped electrodes extended in the z direction as shown in the inset of figure 1. In this case $\alpha = 1 = -\beta$, $\gamma = 0$ (Paul 1990, Leibfried *et al* 2003). The electrodes are set at a potential of $\pm\Phi_0/2$, where $\Phi_0 = 2(V_{dc} + V_{ac}\cos\omega t)$. Thus, $+V_{dc}$ is the DC component applied to the x pair of electrodes and $-V_{dc}$ is the DC component applied to the y pair of electrodes. V_{ac} is the zero to peak amplitude of the rf component oscillating with angular frequency ω.

The resulting electric field is given by its components (Paul 1990)

$$E_x = \frac{-2(V_{dc} + V_{ac}\cos\omega t)}{r_0^2}x,$$
$$E_y = \frac{2(V_{dc} + V_{ac}\cos\omega t)}{r_0^2}y. \qquad (2)$$

The equations of motion of a particle of mass M and charge Q in this field is given by the Mathieu differential equations of motion (Paul 1990).

$$d^2x/d\tau^2 = -(\alpha + 2q\cos 2\tau)x$$
$$d^2y/d\tau^2 = +(\alpha + 2q\cos 2\tau)y \qquad (3)$$

where $\tau = \omega t/2$ and

$$a = 8\frac{Q}{M}\frac{V_{dc}}{r_0^2}\frac{1}{\omega^2}, \qquad q = 4\frac{Q}{M}\frac{V_{ac}}{r_0^2}\frac{1}{\omega^2}. \qquad (4)$$

The parameter $2r_0$ is the shortest distance between two non-adjacent electrode surfaces. The stability of the solution to the equation (3), defining the confining functions of the trap, is dependent on the values of parameters a and q, i.e. the stability depends on the magnitudes of both rf and static components of the applied bias, on the angular rf frequency ω, on the trap dimension r_0, as well as on the ion charge Q over mass M ratio. Figure 1(b) shows the regions of stability for a linear Paul trap. For a nanoscale trap, the dimension r_0 could range from tens of nanometers to a micrometer. As a result, to maintain stability according to equation (4), the other parameters have to adjust resulting in large values for the frequency ranging from a few GHz to a hundreds of MHz. The voltages are limited by the breakdown strength of the medium. As can be seen in figure 1(b), an ion can be stable with application of only AC potential, which has higher breakdown strength than a DC potential. In our modeling of the trap, we have considered potentials varying from 1 to 10 V, frequencies ranging from 400 MHz to 10 GHz, and radius of the trap from 50 to 100 nm.

When $q \ll 1$ and $a \ll 1$, the approximate solution to equation (3) is

$$x(t) \approx x_0\cos(\Omega t + \varphi)\left[1 + \frac{q}{2}\cos(\omega t)\right].$$
$$\Omega \approx \omega\sqrt{a + q^2/2} \qquad (5)$$

Ω is the secular frequency and φ is a phase determined by the initial conditions of position and velocity of the particle. The
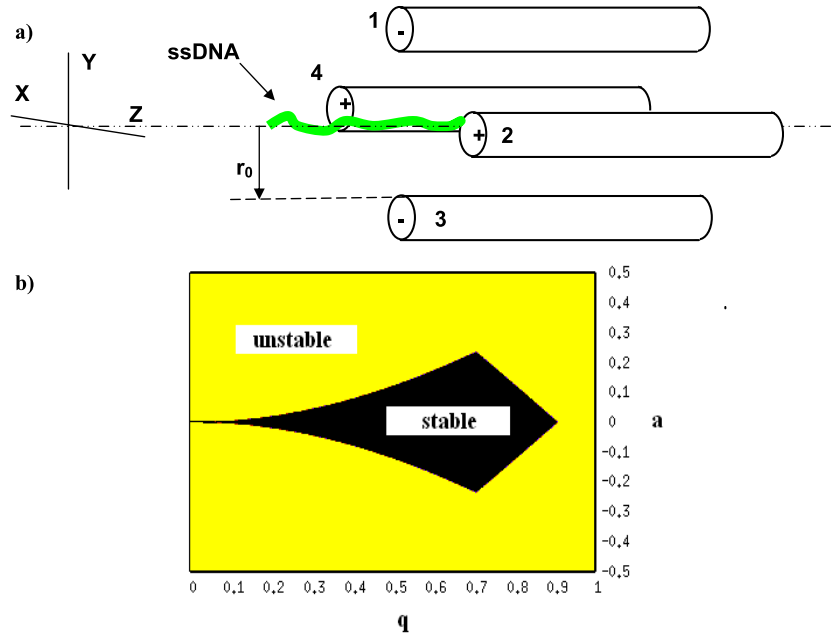
Figure 1. (a) Schematic sketch of a Paul trap, and (b), stability diagram for an ideal 2D Paul trap, showing the ranges of q and a for which the trap is stable.

motion corresponding to $\cos(\omega t)$ term is the micro-motion, driven by the applied ac field. Higher order solutions in powers of q and a contain integer multiple of the frequencies in equation (5).

3. Simulation method

To study the behavior of a bonded line of charges as in a polymer chain or a single stranded DNA, we use a modified version of the molecular dynamics simulation package GROMACS 4.0.5 (Hess *et al* 2008). The forces from the external potential of the quadrupole Paul trap given in section 2 are implemented in GROMACS. The simulations are performed in vacuum with nonperiodic boundary conditions and we ensure that the motion of the center of mass was not removed. The MD simulations for DNA are performed within the NVT (constant number of particles, volume, and temperature) ensemble. The thermostat rescales the velocity with an exponential time constant τ_T but with a stochastic term which ensures a correct kinetic energy distribution (Bussi *et al* 2007).

We first model a linear line of charge by constructing a fictious chain of 267 bounded 'atoms', each of mass of 12 a.m.u and of charge of $1e$. The total chain length is around 40 nm. As far as confinement functions are considered, it turns out that this simplified structure illustrates main features of the realistic ssDNA. The bonds between adjacent atoms $m - m+1$ are assumed in a form of a harmonic potential $V^b(r_{m,m+1}) = \frac{1}{2}k^b(r_{m,m+1} - b_{m,m+1})^2$ where the bond strength was chosen to be $k^b = 38.76$ eV nm^{-2}, and the bond length $b_{lm} = 0.15$ nm (the parameters of a C–C sp^2 bond). The bond angle is defined between vectors connecting adjacent atoms $(m, m-1)$ and $(m, m+1)$, while angular elastic forces are represented by a harmonic potential function $V^\theta(\theta_{lmn}) = \frac{1}{2}k(\theta_m - \theta_m^0)^2$

where k was varied, $k = 0, 0.001$ or 0.01 eV rad^{-2}, with the equilibrium bond angle of $\theta_m^0 = \pi$ rad.

For the ssDNA, a port (Sorin and Pande 2005) of the AMBER03 force field (Duan *et al* 2003) is used. The number of charges on an N sequence DNA is $N - 1$ because one of the phosphate end groups is hydrogen terminated, as follows form the force filed. Unlike in the chain above, the charges are not located on any one atom but are distributed as partial charges on the phosphate groups summing to $-1e$ for each phosphate group (Duan *et al* 2003). Most of our simulations are done for a 60 base ssDNA, though one case is performed with a 180 base ssDNA.

The electrostatic interactions are computed by introducing the Coulomb forces between all particles. This implies that the cut off length for electrostatic potential is larger than the length of the DNA or the chain in all studied cases, thus enabling long-range electrostatic interactions between all charged particles.

Before starting the molecular dynamics simulation the energy minimization of the system is performed with the steepest descent method. A time step in simulations is 1 fs. The neighbor list is updated every time step. For the model chain of beads, the initial velocity is assumed zero, while the initial position is defined with the center of mass of the chain at a fixed distance from the trap center. For the ssDNA of different types and lengths the initial velocity of all atoms is random, obtained from the Maxwell's distribution at 300 K, while the initial position is parallel to the trap axis at a distance (Δx, Δy) from the trap center.

We also tested cases with and without a thermostat for both DNAs and the model chain and found no noticeable difference in the trajectories. In the final simulations no thermostat is used for the chain of beads. However, in the DNA cases we use the velocity-rescaled thermostat (Bussi *et al* 2007). The initial conditions such as center of mass velocity of
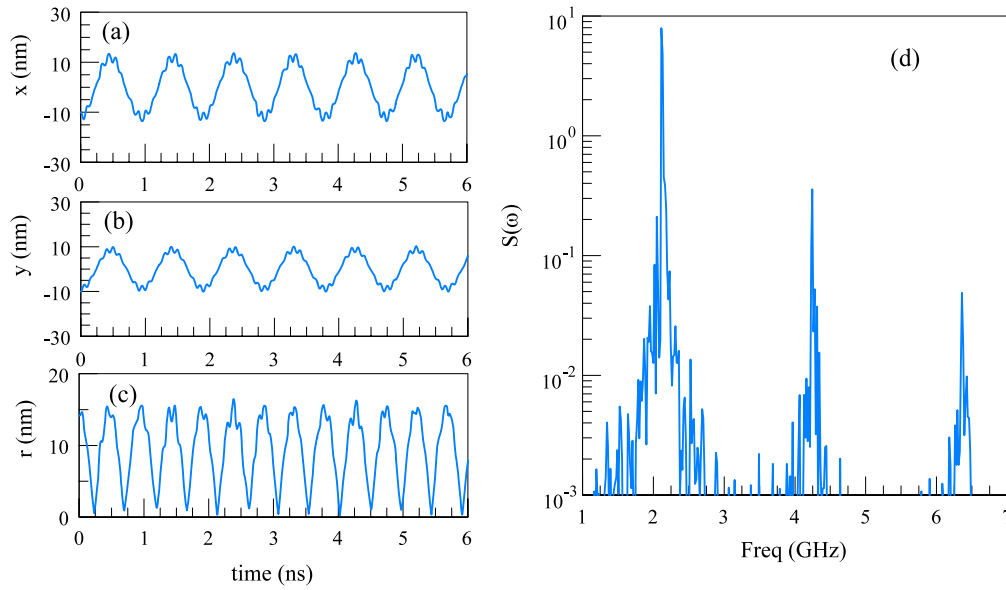
Figure 2. (a) *x*-coordinate, (b) *y*-coordinate, (c) radial distance of a particle from the center of a linear Paul trap. The trap parameters $q = 0.2938$ and frequency $f = 10$ GHz. (d) The PSD $S(\omega)$: the first peak at 2.1 GHz corresponds to the secular oscillation frequency.

the chain or DNA affect the amplitude of the trajectory but not the secular oscillation frequency. Visualization is done using the VMD software (Humphrey *et al* 1996). In most cases, for describing the confinement of a system in the trap, we analyze the radial distance of atoms and the center of mass of a group of atoms from the center of the trap as a function of time.

4. Results and discussion

We compare confinement functions of the linear Paul trap for the cases of a model chain of beads and of ssDNA of different types. For the case of the ssDNA, we compare the trajectory with the standard trajectory of a single ion in the trap. For this reason we first repeat known features of the dynamics of a single particle ion in the Paul trap, which we later use for the comparisons.

4.1. Single particle case

We consider a single charged particle in a Paul trap under the influence of an AC potential ($a = 0$ in equation (4)). The parameter $q = 0.2938$ and frequency $f = 10$ GHz are chosen to mimic the simulation parameters of DNA with the same q-factor in section 4.3. The particle is initially with zero velocity, at $(-9.98, -10.06)$ nm away from the trap center. The equation (5) illustrates a trajectory dependence on the initial conditions. The initial conditions affect only the phase and amplitude of the trajectory. The computed trajectories are shown in figures 2(a) and (b). The power spectral density (PSD) is computed using the radial distance from the trap axis, $r(t)$, defined here as the absolute value of the Fourier transform:

$$S(\omega) = |F_{\mathrm{T}}(\omega)| = \left| \int_{-T/2}^{T/2} r(t)\, e^{-j\omega t}\, dt \right|.$$

The PSD has several peaks, and the three most prominent ones are shown in figure 2(d). From equation (5), the secular

oscillation frequency for $a = 0$, $\Omega \approx \omega q / \sqrt{2} = 2.1$ GHz. The first peak corresponds to the secular oscillation. Larger peaks are integer multiple of Ω.

4.2. Chain of charged beads

In order to understand the behavior of a line charge in comparison with a single charged particle in a linear Paul trap, we consider a chain of charged atom-like particles. Two different initial positions were considered: (i) with the chain initially parallel to the z-axis at a distance of $(\Delta x, \Delta y) = (10, 20)$ nm from the z-axis of the trap, (ii) the chain initially straight but slanted by an angle of $10°$ to the z-axis. The applied parameters of the Paul trap are $V_{ac} = 0.8$ V, $V_{dc} = 0$, $r_0 = 100$ nm, and $f = 10$ GHz, which yields for beads $q \approx 0.65$.

Figure 3(a) shows the trajectory of a chain with $k = 0.01$ eV rad^{-2}. As long as the initial position of the chain is parallel to the z axis, the chain remains parallel regardless of the angular bond strength k. As a consequence, peaks of the PSD for various k have the same location and width (figure 3(b)). The chain behaves as a rigid rod regardless of k. Only the range of frequencies corresponding to the secular oscillation (≈ 5.1 GHz) is shown, and it is very close to the case of a single particle. The motions of the centers of mass of the chains with various angular force constants and with an initial orientation of $10°$ about the x-axis is shown in figure 3(c). The center of mass trajectories are almost the same for different bond strengths in figure 3(a) with overlapping trajectories for all three cases but the fluctuations and oscillations are different such that the actual atom positions do not overlap for various k values. After about 4 ns from the start of the simulation, some of the atoms of the most rigid chain ($k = 0.01$), went beyond the trap geometry (radial position $> r_0$), pulling the others and leading to the unstable trajectory. The smaller k means larger flexibility of the chain, and each of the atoms try to confine independently. However, large $k = 0.01$ eV rad^{-2}
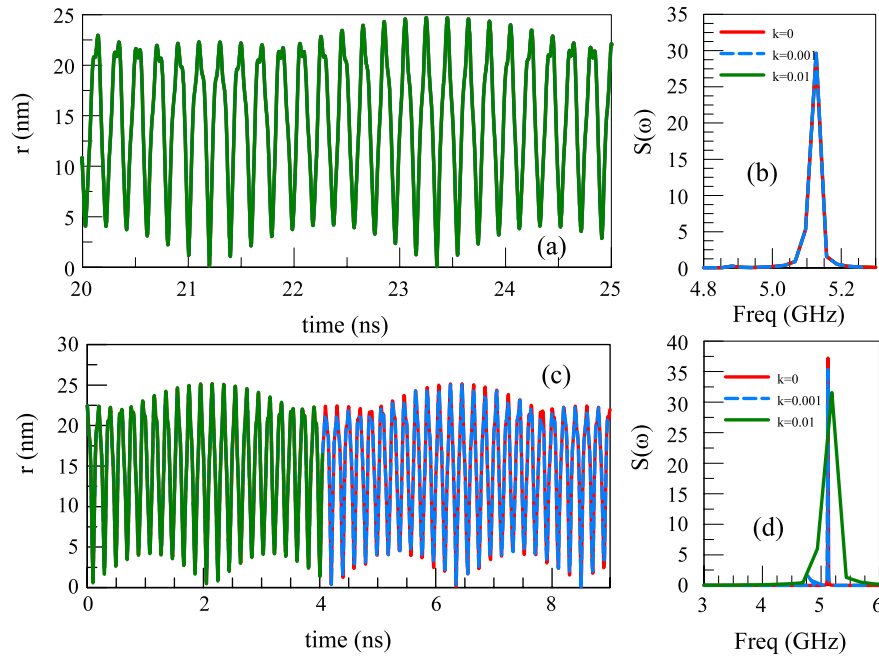
Figure 3. (a) The motion of the center of mass of a chain initially parallel to the z-axis for bond angle force constant of $k = 0.01$ eV rad^{-2}. (b) The power spectral density of the center of mass trajectories for different harmonic bond angle force constants $k = 0, 0.001$ and 0.01 eV rad^{-2} for the trajectories in (a), showing overlapping trajectories. (c) The motion of the center of mass of the chains of various angular force constants with the initial orientation at an angle to the trap axis. The trajectories overlap except for $k = 0.01$ eV rad^{-2} which becomes unstable after 4 ns. (d) The PSD of the center of mass trajectories for different harmonic bond angle strengths $k = 0, 0.001, 0.01$ eV rad^{-2} for the trajectories in (c).
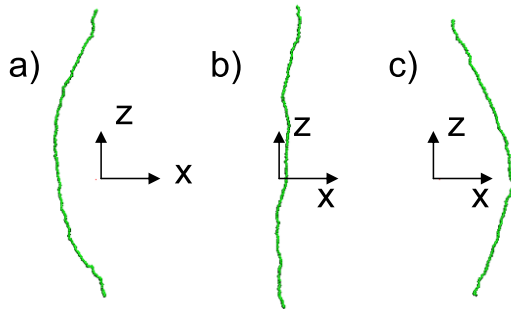

Figure 4. (a)–(c) are different conformations of the chain as it oscillates in the trap. The z-axis is the trap axis. The bending is a result of the initial orientation, which is here 10° to the z-axis, while $k = 0$.

yields a high degree of correlation of atomic motion, and the chain behaves close to a rigid rod. Difference of the forces to the various atoms along the rod produces a torque that rotate the whole system and eventually the end atoms might leave the trap radius if the chain is long enough. Note that PSD for the unstable case is obtained by integration up to 4 ns only, leading to apparently broader peak as compared to the other two cases (figure 3(d)). From figures 3(b) and (d) the secular frequency of the chain center of mass is $\Omega \approx 5.1$ GHz in figure 3 is not too far form the estimated frequency $\Omega_0 \approx 4.65$ GHz of the single ion in a trap with the same q factor (0.65).

Furthermore, if the initial position of the chain is not parallel to the trap axis but is inclined by an angle, the chain fluctuates and bends (figure 4), since various atoms, being at different distances form the trap axis are under different

electrical forces of the trap. In figure 5, the rotations and oscillations of the chain are quantified by plotting the variation with time of the angle between a line joining the center atom of a chain and top end (at figure 4) with respect to the trap axis for various k. For the chain with weaker bond strength, the oscillations are relatively small, but when the tube is most rigid ($k = 0.01$), the tube undergoes a few rotations, and even flipping the orientations, before becoming unstable (figure 5(c)). When the chain of atoms is most rigid (largest k) the chain undergoes complete rotation before one of the atoms exceeds r_0 and the trajectory becomes unstable. We note that the bond strength, k_b, is kept the same in all cases because it does not influence the flexibility of the chain, critical for the stability in the trap. Size of k_b rather modifies the stretching of the chain, which might modify its length but is not critical in the confinement.

4.3. Single stranded DNA

Unlike the chain of point charges considered in section 4.2, an ssDNA is geometrically a more complex system. Thus, the atoms of the DNA bases extend about a nm from the axis, and could carry their own electrostatic charges. Besides, point charges are not distributed uniformly in the DNA but are rather distributed as partial charges. Finally, the bonding characteristics of a DNA are distributed and more complex than in the case of our modeled chain bonding. The following types of the ssDNA are considered: (i) 60 base ssDNA, with identical bases of G, A, T and C type, (ii) a 60 base ssDNA with mixed 15G-15A-15T-15C type, (iii) a 180 base single stranded DNA, by lining up 3 ssDNAs of case (ii), and (iv) a
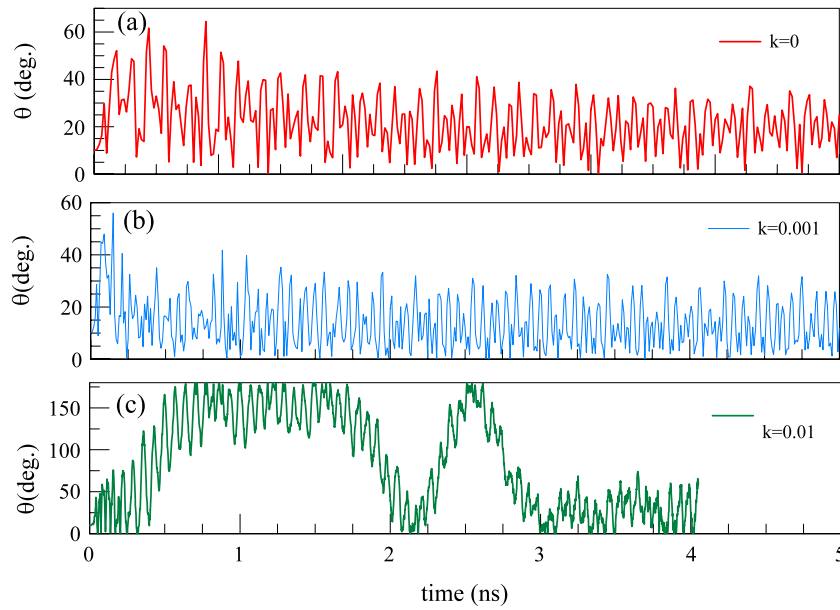
Figure 5. (a)–(c) The variation of the angle between a line joining the center atom of a chain and one of the ends with respect to the trap axis for different flexibilities as a function of time.

60 base ssDNA with randomly mixed bases. The initial length of the 60 base ssDNA is approximately 40 nm. The DNA is constructed as a single strand of a helical DNA that retains a small pitch. Initially, the helical DNA axis is parallel to the trap axis. During the initial, preparation phase of the simulation the ssDNA straightens out from the initial helical coil, but not necessarily fully parallel to the trap axis. We note that due to the spatial, unaligned, distribution of the charges in a ssDNA, together with the described geometrical fluctuations leads to unequal trap electrical forces to various atoms and monomers of the ssDNA.

4.3.1. Comparison of DNA trajectory and a single particle trajectories. Under the conditions of $V_{ac} = 10$ V, $V_{dc} = 0$. $f = 10$ GHz, $r_0 = 100$ nm ($q = 0.2938$, as in section 4.1), a 60 base DNA with only G bases is stable. The initial position of the center of mass is $(-9.98, -10.06)$ nm from the axis of the trap. The atoms of the DNA have a Maxwellian velocity distribution at 300 K. Though the DNA is initially parallel to the trap axis, it undergoes rotations and can be inclined to the z-axis as illustrated in the snapshot in figure 6. Though the DNA does not remain parallel to the z-axis, we note that the DNA does not curl up into a ball.

The charge–mass ratio Q/M for a ssDNA is calculated by dividing the total charge by the total mass. The stable trajectories of the DNA are shown in figure 7 above. Figure 7(a) shows the trajectories of the end groups along with that of the center of mass. The figure shows that the oscillations of the end groups are in opposite phases. In figures 7(b)–(d) the comparison of the center of mass DNA trajectory with that of particle having the same q-factor of 0.2938 is presented. It is remarkable that a single particle and a DNA with a complex structure with distributed charges have very similar trajectories, as is further illustrated by the overlapping PSDs in figure 7(f).
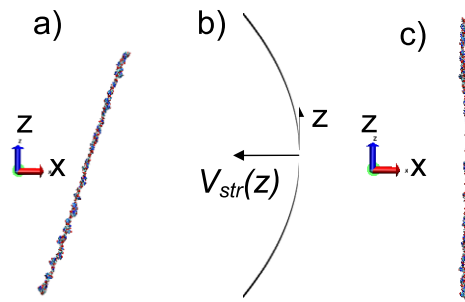

Figure 6. (a) A snapshot of a 60 G base ssDNA as it oscillates in the trap. The z-axis denotes the trap axis. The DNA remains straight though it undergoes some oscillations and is not parallel to the z-axis. (b) A schematic of a parabolic stretching potential that could be applied in the z-direction to confine the DNA (c) DNA position after stretching potential is applied.

4.3.2. Comparison the trajectories of ssDNAs of various types. We compare the trajectories of 4 different 60 base ssDNA, defined by G, A, T or C bases. Two cases are tested: with ($V_{dc} = 0.02$ V, $V_{ac} = 1$ V, $r_0 = 50$ nm, $f = 5$ GHz) and without dc voltage ($V_{dc} = 0$). The 50 ns sections of the r coordinate of the trajectories are shown in figures 8(a)–(c). The trajectories have similar features, yet they are not identical and do not overlap each other.

In order to capture the differences in the trajectories, we computed the Fourier transform of these trajectories, shown in figures 8(d)–(f). For the ssDNAs with identical bases throughout, the PSD peaks are clearly distinguishable when varying the type. The peaks are related to the secular oscillation frequency. In figure 8(e), the power spectrum for a single charged particle in the 2D Paul trap with the same q-factor for each DNA base is shown in dashed lines, showing a strong mutual correlation This implies that the
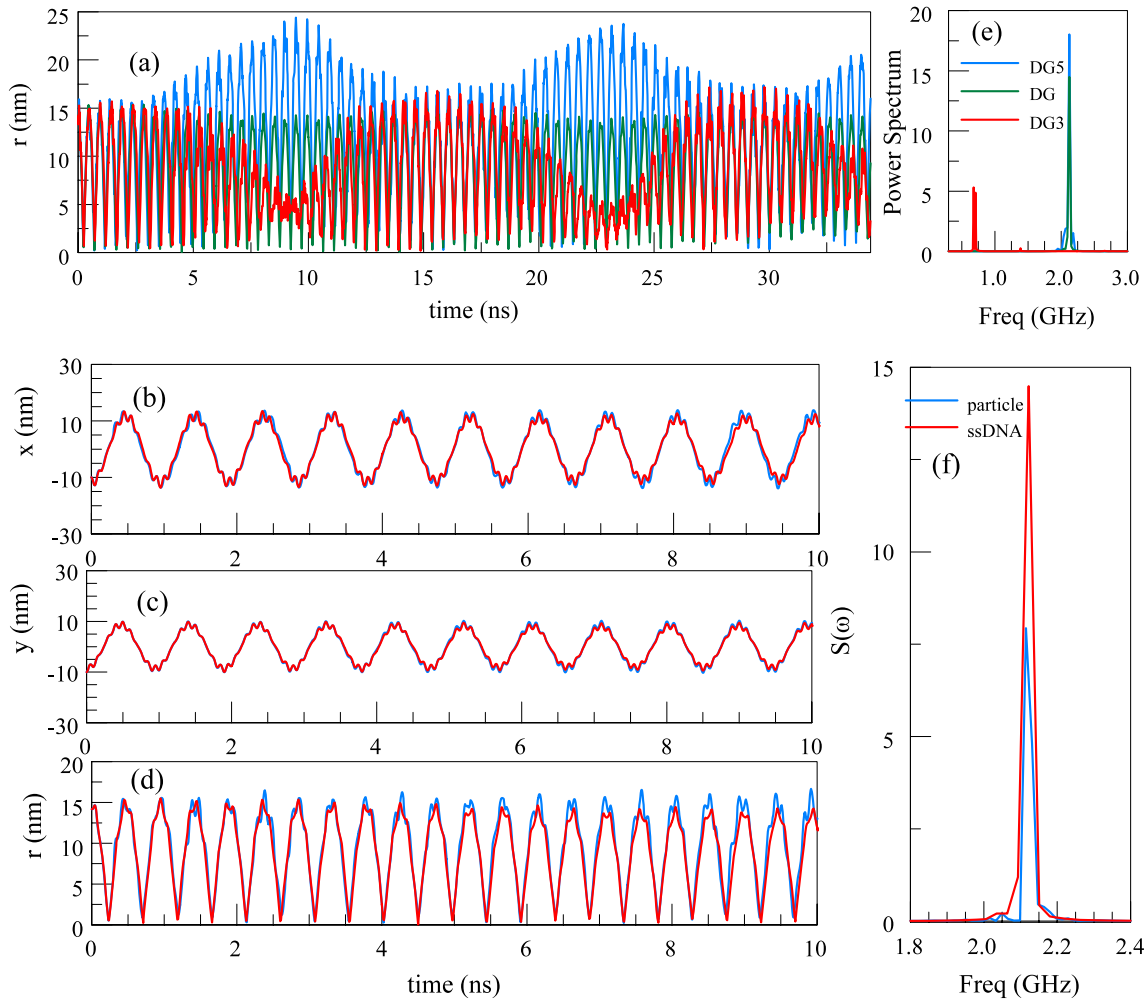
Figure 7. (a) *r* trajectory of the center of mass (green) as well as the center of mass of the end groups (red and blue) as a function of time. (b)–(d) are *x*, *y* and *r* coordinates of the trajectories of a 60 G base ssDNA as a function of time, compared with the trajectory of a single particle. (e) PSD for the center of mass of the DNA as well as the center of mass of the end groups denoted by DG5 and DG3. (f) Comparison of the center of mass PSD for the ssDNA with that of a particle with the same *q*-factor.

DNA structure, charge distribution, bond parameters etc do not significantly influence the power spectrum of the center-of-mass trajectory of the DNA. It is the charge–mass ratio that primarily determines the location of the peaks. In figure 8(f), the power spectrum of the trajectory of an ssDNA with 15 contiguous bases of G, A, T, and C is shown. The main peak (secular frequency) at ~1.9 GHz of the C-segment (green) overlaps with the peak of the neighboring T-segment (blue), and is not visible at the figure. The main peak of the A-segment, neighboring T, is also approximately at 1.9 GHz. Thus, C, T and A segments show a strong motion correlation influencing a common secular frequency, different form the individual ones. The exception is the G-segment, which tries to remain its own secular frequency (as in (e)), though broadened and split.

4.3.3. Mixed base DNA. We consider a 60 base DNA with a mixed sequence (15G, 15A, 15T, 15C). The *r*(*t*) coordinate of the trajectories of the center of mass of individual bases are plotted in figure 9. The end bases motion are DC5 and DG3.

Two interior chosen bases are also considered (the base DA is located towards the end of DNA with the end group DC5 and DC is located towards the end with base DG3). The trajectories and the PSD (figure 9(b)) show that motion correlation caused by geometrical proximity of the various segments is a major factor in the similarity of the trajectories and the relevant spectral densities. For example DC5 and DC are both Cytosine bases but their spectral densities are markedly different. DC5 and DA have similar characteristics and DC and DG3 have common peaks arising from geometrical proximity.

4.3.4. Application of the stretching potentials. Just as in a chain of beads, ssDNA exhibits oscillations. In figure 10(a) we show the variation with time of the angle between the trap axis and the line connecting the center of mass of the end groups of a 60 base G ssDNA of the *q*-factor = 0.47 (V_{ac} = 4 V, r_0 = 100 nm, f = 5 GHz). The angle varies roughly between 0° and 45°. In order to stabilize DNA translocation through the Paul trap, it is important to suppress these oscillations.

Here we propose a stretching field in the axial *z* direction, $E_{str} = 0.1((z - z0)/L)$ V nm^{-1} where *L* is the length of
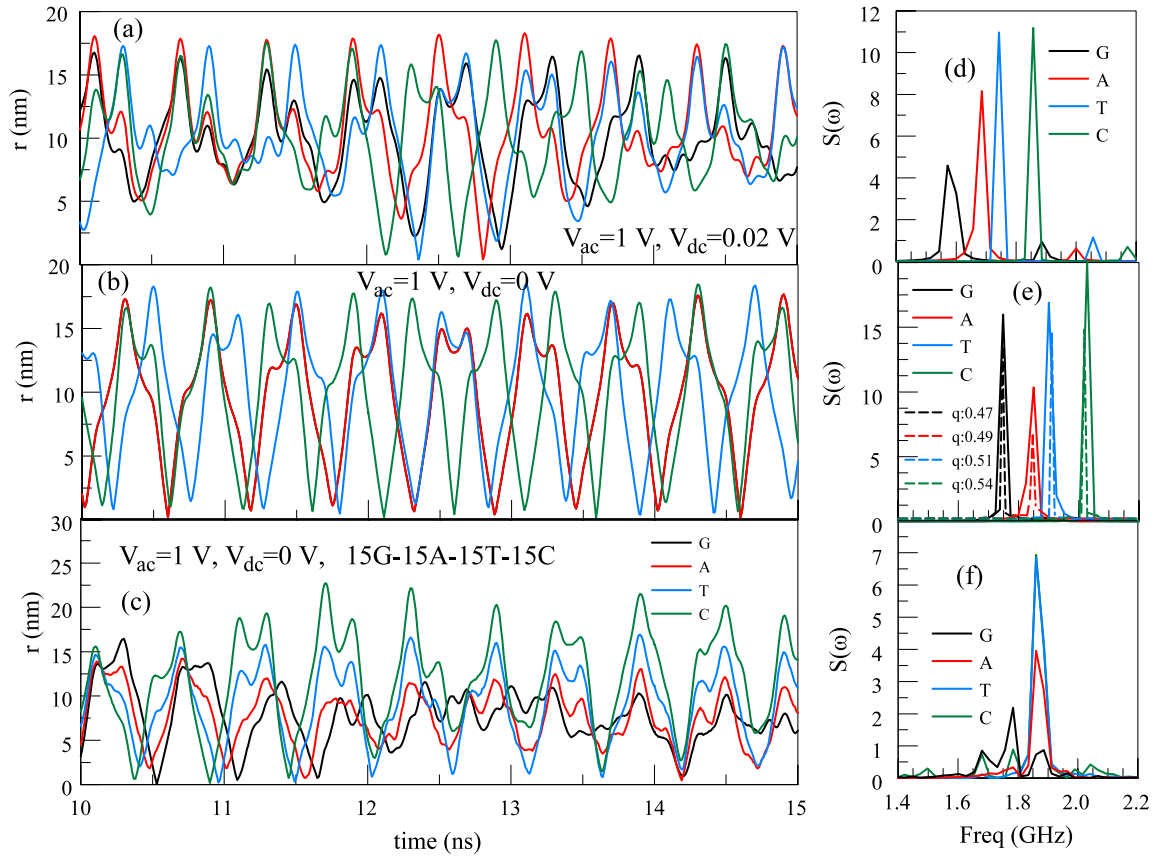
Figure 8. (a) $r(t)$ coordinate of trajectory of the center of mass of ssDNAs with different bases with $V_{dc} = 0.02$ V, and (b) $r(t)$ of the center of mass for $V_{dc} = 0$ V. (c) The $r(t)$ of center of masses of G, A, T, C of a 60 base ssDNA with 15 contiguous bases of G, A, T and C. (d) PSD of a 60 base, ssDNA in (a). (e) The PSD for case in (b). Also shown in dashed lines is the PSD of the r(t) for a single particle with different q-factors corresponding to different DNA bases. (f) The PSD for case (c).
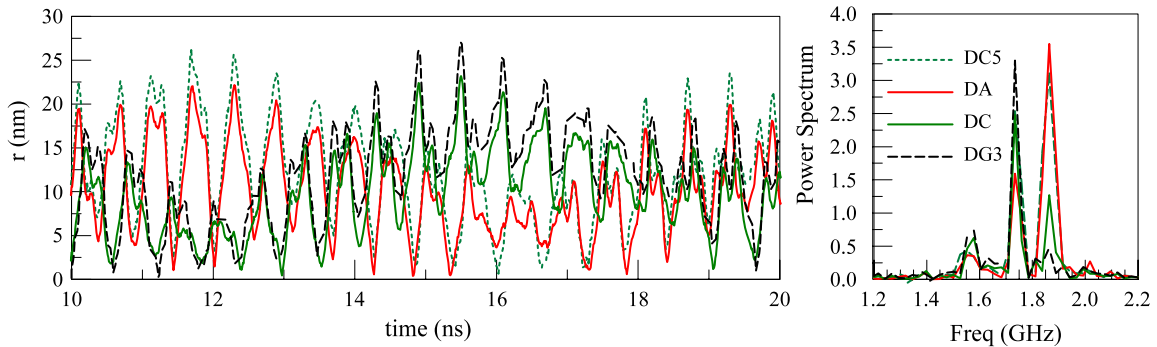

Figure 9. (a) r trajectory of the center of mass of two end bases (DC5 and DG3) and two interior bases (DA and DC) in a mixed base ssDNAs consisting of 60 bases; $V_{dc} = 0$ V, $V_{ac} = 1$ V, $r_0 = 50$ nm, $f = 5$ GHz and (b) the PSD of the center of mass of the bases.

a DNA, z is the z coordinate of the atom, $z0$ is the mean z coordinate of all atoms. The electrostatic potential is parabolic as shown in figure 6(b). Clearly from the figure the stretching field reduces the rotation around the z-axis such that the range of angles is reduced from 0°–40° to 0°–8° and orients the DNA parallel to the trap axis.

4.3.5. Stability range of an ssDNA. The center of mass motion can be used to define the stability of an ssDNA in the Paul nanotrap. From the considerations in this section it

follows that the range of stability for an ssDNA for various $q - a$ values is similar to that of a single ion shown in figure 1(b). For a case of $V_{ac} = 1$ V, $r_0 = 100$ nm, $f = 1$ GHz, $q \approx 2.8$, the ssDNA center-of-mass trajectory was unstable as is expected for a single ion for the same q factor. However in some cases, close to the boundaries of the range of stability in figure 1(b), where one would find the stability for a single ion, the ssDNA is unstable. For example, we considered a case near the edge of the stable region in figure 1(b) where $q = 0.47$ and $a = 0.94$. Although for a single ion this
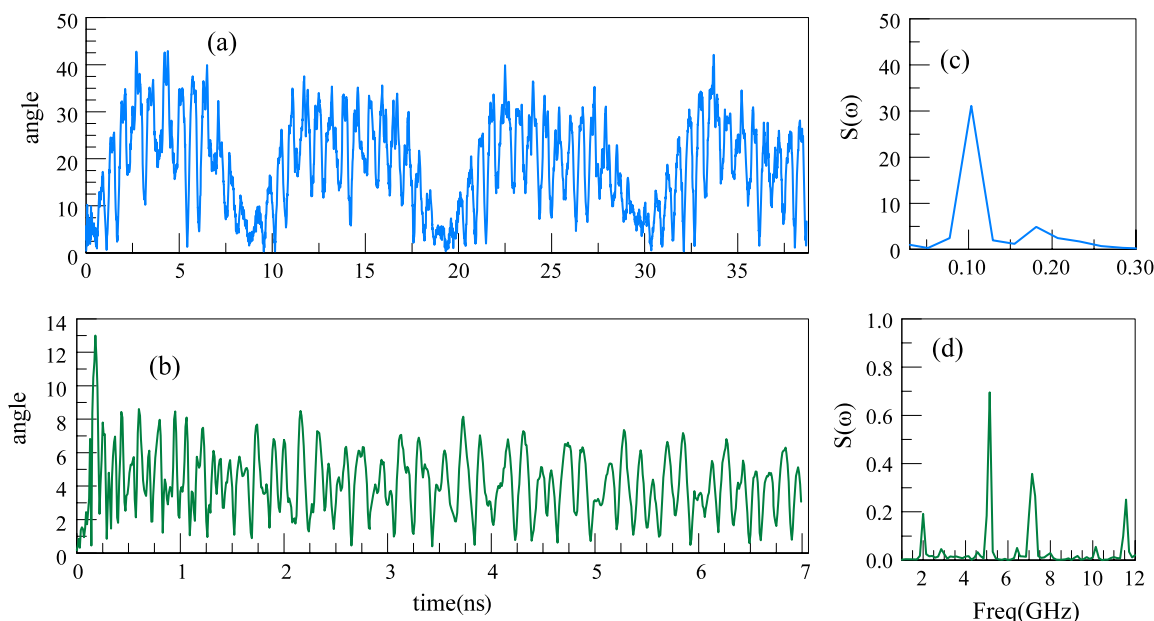
Figure 10. Shown are the variations with time of the angle of the line connecting the end bases with the *z*-axis. (a) 15 bases of G, 15A, 15C, 15T. (b) The variation of the angle for an ssDNA with 180 bases (replicated the DNA above 3 times) but with the stretching field. Corresponding power spectral densities are shown at (c) and (d).

would give a stable trajectory, for a 60 G base DNA, with $V_{dc} = 0.08$ V, $V_{ac} = 1$ V, $r_0 = 50$ nm, $f = 5$ GHz we obtained an unstable trajectory already after about 0.3 ns (at least one atom had an *r*-coordinate greater than r_0). This is caused by additional degrees of motion of the ssDNA, spatial distribution of its charges, as well as by a random nature of initial conditions of various atoms in the DNA, subject to the Maxwell distribution of velocities.

Coulomb force couple normally decoupled various degrees of freedom in the linear Paul trap, thus complicating the problem to the coupled Mathieu equations, leading to the effects of the locking of the secular frequencies of the two particle, reducing the size of the confinement region, etc. A nice analysis of such a case (in presence of a dissipative medium) is given in Hoffnagle and Brewer (1994) for a case of Coulomb coupling between two particles in a dissipating medium. The cases considered here, even in case of chain of charged beads, are more complicated for a several reasons: existence of the Coulomb forces between all charged particles in the polymer (leading to a large number of coupled equations), combined with variety of harmonic forces between all neighboring particles (various atoms). Thus, bonds between the atoms cause additional restrains on the motion of the particles, such that the motion of the system of particles resembles to the motion of a single charged body.

5. Conclusions

Using molecular dynamics simulations, we have studied the dynamics of a filamented structure with line-distributed charges such as a charged linear polymer and a single stranded DNA in a nanoscale 2D Paul trap, in vacuum. A line charge can be effectively trapped, with stability parameters similar in

values to the single charged particle of the same Q/M ratio (figures 1(b) and 2). A line charge undergoes both oscillations and rotations in the trap depending on its initial angle, position and velocity, as well as of the angular bonding force of the adjacent atoms. A 40 nm long single stranded DNA does not fold or curl in the Paul trap, but could undergo rotations and oscillations about the center of mass, similarly to the chain of charges. Application of a stretching force by the gradient electric field suppresses the rotations, and stabilizes the DNA confinement in the linear trap.

So far, we have constructed a preliminary version of the Paul trap (with center gap regions of the order of microns) and demonstrated operation and stability similar to that discussed here. The full description of the experimental realization, and the scaling to dimensions discussed here, will appear in subsequent publications.

References

Abich K, Keil A, Reiss D, Wunderlich C, Neuhauser W and
    Toschek P E 2004 Thermally activated hopping of two ions

trapped in a bistable potential well *J. Opt. A: Pure Appl. Opt.* B **6** S18–23

Aksimentiev A, Heng J B, Timp G and Schulten K 2004a Microscopic kinetics of DNA translocation through synthetic nanopores *Biophys. J.* **87** 2086–97

Aksimentiev A, Schulten K, Heng J, Ho C and Timp G 2004b Molecular dynamics simulations of a nanopore device for DNA sequencing *Biophys. J.* **86** 480A–A

Arnott D, Henzel W J and Stults J T 1998 Rapid identification of comigrating gel-isolated proteins by ion trap mass spectrometry *Electrophoresis* **19** 968–80

Branton D *et al* 2008 The potential and challenges of nanopore sequencing *Nat. Biotechnol.* **26** 146–53

Bussi G, Donadio D and Parrinello M 2007 Canonical sampling through velocity rescaling *J. Chem. Phys.* **126** 014101

Chen C M 2005 Driven translocation dynamics of polynucleotides through a nanopore: off-lattice Monte Carlo simulations *Physica* A **350** 95–107

Chen C M and Peng E H 2003 Nanopore sequencing of polynucleotides assisted by a rotating electric field *Appl. Phys. Lett.* **82** 1308–10

Duan Y *et al* 2003 A point-charge force field for molecular mechanics simulations of proteins based on condensed-phase quantum mechanical calculations *J. Comput. Chem.* **24** 1999–2012

Edwards C S, Gill P, Klein H A, Levick A P and Rowley W R C 1994 Laser-cooling effects in few-ion clouds of YB$^+$ *Appl. Phys.* B **59** 179–85

Fredlake C P, Hert D G, Mardis E R and Barron A E 2006 What is the future of electrophoresis in large-scale genomic sequencing? *Electrophoresis* **27** 3689–702

Healy K 2007 Nanopore-based single-molecule DNA analysis *Nanomedicine* **2** 459–81

Hess B, Kutzner C, van der Spoel D and Lindahl E 2008 GROMACS 4: algorithms for highly efficient, load-balanced, and scalable molecular simulation *J. Chem. Theory Comput.* **4** 435–47

Hoffnagle J J and Brewer R G 1994 *Science* **265** 213

Howorka S, Cheley S S and Bayley H 2001 *Nat. Biotechnol.* **19** 636

Humphrey W, Dalke A and Schulten K 1996 VMD: visual molecular dynamics *J. Mol. Graphics* **14** 33

Itano W M, Bergquist J C, Bollinger J J and Wineland D J 1995 Cooling methods in ion traps *Phys. Scr.* T **59** 106–20

Kasianowicz J J, Brandin E, Branton D and Deamer D W 1996 *Proc. Natl Acad. Sci. USA* **93** 13770

Kricka L J, Park J Y, Li S F Y and Fortina P 2005 Miniaturized detection technology in molecular diagnostics *Expert Rev. Mol. Diagnos.* **5** 549–59

Lagerqvist J, Zwolak M and Di Ventra M 2006 Fast DNA sequencing via transverse electronic transport *Nano Lett.* **6** 779

Lagerqvist J, Zwolak M and Di Ventra M 2007 Influence of the environment and probes on rapid DNA sequencing via transverse electronic transport *Biophys. J.* **93** 2384–90

Leibfried D, Blatt R, Monroe C and Wineland D 2003 Quantum dynamics of single trapped ions *Rev. Mod. Phys.* **75** 281–324

Nakane J J, Akeson M and Marziali A 2003 Nanopore sensors for nucleic acid analysis *J. Phys.: Condens. Matter* **15** R1365–93

Oberacher H, Parson W, Oefner P J, Mayr B M and Huber C G 2004 Applicability of tandem mass spectrometry to the automated comparative sequencing of long-chain oligonucleotides *J. Am. Soc. Mass Spectrometry* **15** 510–22

Paul W 1990 Electromagnetic traps for charged and neutral particles *Rev. Mod. Phys.* **62** 531–40

Payne C M, Zhao X C, Vlcek L and Cummings P T 2008 Molecular dynamics simulation of ss-DNA translocation between a copper nanoelectrode gap incorporating electrode charge dynamics *J. Phys. Chem.* B **112** 1712–7

Rhee M and Burns M A 2006 Nanopore sequencing technology: research trends and applications *Trends Biotechnol.* **24** 580–6

Rhee M and Burns M A 2007 Nanopore sequencing technology: nanopore preparations *Trends Biotechnol.* **25** 174–81

Rothbauer U, Zolghadr K, Muyldermans S, Schepers A, Cardoso M C and Leonhardt H 2008 A versatile nanotrap for biochemical and functional studies with fluorescent fusion proteins *Mol. Cell. Proteomics* **7** 282–9

Ryan D, Rahimi M, Lund J, Mehta R and Parviz B A 2007 Toward nanoscale genome sequencing *Trends Biotechnol.* **25** 385–9

Schiffer J P 2003 Order in confined ions *J. Physique* B **36** 511–23

Seidelin S *et al* 2006 Microfabricated surface-electrode ion trap for scalable quantum information processing *Phys. Rev. Lett.* **96** 253003

Shi L, Zhu X W, Feng M and Fang X M 1999 Ordered structures of a few ions in the Paul trap *Commun. Theor. Phys.* **31** 491–6

Sorin E J and Pande V S 2005 Exploring the helix–coil transition via all-atom equilibrium ensemble simulations *Biophys. J.* **88** 2472–93

Tabard-Cossa V, Trivedi D, Wiggin M, Jetha N N and Marziali A 2007 Noise analysis and reduction in solid-state nanopores *Nanotechnology* **18** 305505

Trepagnier E H, Radenovic A, Sivak D, Geissler P and Liphardt J 2007 Controlling DNA capture and propagation through artificial nanopores *Nano Lett.* **7** 2824–30

Tsai Y S and Chen C M 2007 Driven polymer transport through a nanopore controlled by a rotating electric field: off-lattice computer simulations *J. Chem. Phys.* **126** 144910

Vant K, Chiaverini J, Lybarger W and Berkeland D J 2006 Photoionization of strontium for trapped-ion quantum information processing arXiv:quant-ph/0607055

Walther H 1995 From a single-ion to a mesoscopic system—crystallization of ions in Paul traps *Phys. Scr.* T **59** 360–8

Wineland D J, Monroe C, Itano W M, Leibfried D, King B E and Meekhof D M 1998 Experimental issues in coherent quantum-state manipulation of trapped atomic ions *J. Res. Natl Inst. Standards Technol.* **103** 259–328

Zhang X G, Krstic P S, Zikic R, Wells J C and Fuentes-Cabrera M 2006 First-principles transversal DNA conductance deconstructed *Biophys. J.* **91** L4–6

Zhao X C and Krstic P S 2008 Molecular dynamics simulation study on trapping ions in a nanoscale Paul trap *Nanotechnology* **19** 195702

Zhao X C, Payne C M, Cummings P T and Lee J W 2007 Single-strand DNA molecule translocation through nanoelectrode gaps *Nanotechnology* **18** 424018

Zikic R, Krstic P S, Zhang X G, Fuentes-Cabrera M, Wells J and Zhao X C 2006 Characterization of the tunneling conductance across DNA bases *Phys. Rev.* E **74** 011916

Zwolak M and Di Ventra M 2005 Electronic signature of DNA nucleotides via transverse transport *Nano Lett.* **5** 421